JCRS

Journal of Chemical Reactivity and Synthesis 2025: 15(2) 148-162

Research Article

Experimental Investigation of Viscosity and Thermal Coefficients Affecting Heat Transfer in Crude Oil Blended with Ferric oxide Nanoparticles to Determine Its Thermophysical Properties

Akbar Darvishi

Department of Chemical Engineering, Fir.C., Islamic Azad University, Firoozabad, Iran

ABSTRACT

This study investigates the influence of incorporating nanosized Ferric oxide (Fe_2O_3) particles into crude oil on its thermophysical and hydrodynamic properties. Experimental analyses were conducted using a custom-designed system consisting of an adiabatic test section, a heating unit, and a control module to evaluate variations in viscosity, density, thermal conductivity, thermal diffusivity, and flow behavior. Samples of crude oil were blended with different weight fractions of Ferric oxide nanoparticles (1–11 wt%) and tested under temperatures ranging from 25 to 90 °C. The results revealed that adding nanoparticles significantly enhanced thermal conductivity (by up to 2.48 times) and overall heat transfer coefficient (by approximately 1.5 times) compared to the base crude oil. Conversely, properties such as kinematic viscosity and Prandtl number decreased with increasing temperature and nanoparticle loading. Experimental findings indicated that nano-enhanced oils exhibited higher Reynolds and Peclet numbers, faster flow velocities, and a moderate increase in friction factor. These outcomes demonstrate the potential of Ferric oxide nanoparticles to improve the heat transfer characteristics of crude oil, making them promising candidates for advanced thermal management and efficient energy transport in petroleum processing and pipeline systems.

ARTICLE INFO

Received: 28 October 2025
Accepted: 15 January 2026
Available: 30 January 2026

✉: A. Darvishi
Akbardarvishi@iau.ac.ir

10.82437/jcrs.2025.1222706

Keywords: Nanoparticles; Thermophysical properties; Hydrodynamics; Viscosity; Ferric oxide.

Introduction

In recent years, nanotechnology has emerged as a transformative approach across various engineering fields, particularly in energy systems, owing to its ability to alter material properties at the nanoscale [1]. One of its most important applications involves modifying conventional fluids through the dispersion of nanoparticles to create *nanofluids*, which have attracted significant attention [2]. Nanofluids exhibit enhanced thermal conductivity, modified rheological characteristics, and superior heat transfer performance compared with

their base fluids, making them highly attractive for use in heat exchangers, oil transport systems, and enhanced oil recovery processes [3].

Among metal oxides, Ferric oxide (Fe_2O_3) nanoparticles have drawn particular interest due to their catalytic and thermophysical advantages [4]. Their high surface-to-volume ratio and intrinsic thermal conductivity enable more effective interactions with the host fluid [5]. Despite extensive studies on other metal oxide nanoparticles such as Al_2O_3 and TiO_2, the effect of nanoscale Ferric oxide on crude oil systems has not been comprehensively examined—especially under the dynamic temperature and flow conditions associated with industrial pipelines [6].

Crude oil, a viscous and typically dark-colored liquid formed from the remains of ancient marine organisms over millions of years, is a vital natural resource often referred to as *"black gold."* Found in subsurface sedimentary rock formations and seabeds, crude oil is a complex mixture of thousands of chemical compounds, primarily hydrocarbons—molecules composed of carbon and hydrogen atoms [7-9]. In addition, crude oil contains small amounts of sulfur, nitrogen, and heavy metals [10].

Given its composition and thermal behavior, crude oil's properties can be significantly influenced by nanoparticle additives [11]. Ferric oxide nanoparticles, with their favorable surface chemistry and thermal conductivity, can enhance the interaction between particles and the fluid matrix [12]. However, a detailed assessment of their effects under realistic flow and temperature conditions remains limited [13].

This study addresses this knowledge gap by experimentally investigating the influence of Ferric oxide nanoparticle additives on the thermophysical and flow characteristics of light crude oil. The results are expected to contribute to the development of efficient crude oil

transportation systems, improved thermal management, and the integration of nanotechnology into modern petroleum engineering practices.

2. Materials and Methods

2.1. Materials

In this study, light crude oil obtained from a domestic refinery was used as the base fluid. The nanoparticles employed were ferric (III) oxide (Fe_2O_3) with an average particle size of 20–40 nm and purity greater than 99.5%, supplied by *Sigma-Aldrich*. The physical properties of crude oil and Fe_2O_3 nanoparticles are summarized in Table 1.

Table 1. Weight characteristics of crude oil.

API	Fluid type
30.83	Crude oil

To ensure proper dispersion and stability of the nanoparticles within the crude oil, a two-step preparation method was applied. Initially, the required mass of Fe_2O_3 nanoparticles was measured to achieve weight fractions ranging from 1% to 11%. The nanoparticles were gradually added to the crude oil under continuous mechanical stirring at 1000 rpm for 45 minutes, followed by ultrasonic homogenization for 30 minutes to prevent agglomeration and ensure uniform dispersion.

2.2. Experimental Setup

A custom-designed thermal test loop was constructed to evaluate the hydrodynamic and thermophysical performance of the crude oil–nanoparticle mixtures. The experimental system consisted of three primary sections:

1. Adiabatic test section,
2. Heating unit, and
3. Measurement and control module.

A schematic diagram of the setup is presented in Figure 1. The test section was fabricated from stainless steel tubing with an inner diameter of 25 mm and a total length of 1.2 m, insulated with glass wool to minimize heat losses. Electrical heating was provided by a nichrome wire element (2 kW capacity) wound uniformly around the test section, allowing precise temperature control through a digital PID controller.

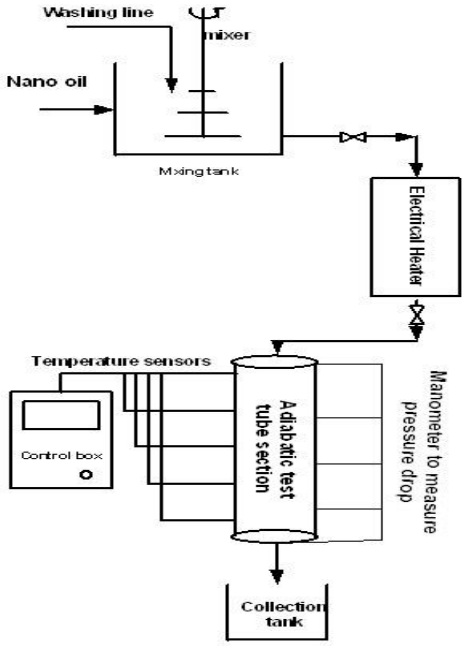

Fig. 1. Schematic of the process under study.

Thermocouples (type K, accuracy ±0.1 °C) were installed at the inlet, outlet, and five intermediate positions along the test section to record the temperature distribution. Pressure was monitored using digital pressure transducers (range: 0–500 kPa), while volumetric flow rate was measured by a rotameter calibrated for oil–nanoparticle mixtures. The system allowed adjustment of both mass flow rate and heating power, enabling experiments under various thermal and hydrodynamic conditions.

2.3. Measurement Procedures

Each experiment was performed under steady-state conditions. The system was initially operated with pure crude oil to establish baseline data. Then, Fe_2O_3 nanoparticle suspensions were tested sequentially at concentrations of 1, 3, 5, 7, 9, and 11 wt%, with operating temperatures of 25, 45, 65, and 90 °C.

The following parameters were measured or calculated during each run:

- Dynamic viscosity (μ) using a rotational viscometer (Brookfield DV-II Pro),
- Density (ρ) using a digital densitometer,
- Thermal conductivity (k) via a KD2 Pro thermal properties analyzer,
- Specific heat capacity (Cp) using a differential scanning calorimeter (DSC),
- Flow rate, pressure drop, and temperature difference across the test section.

Thermal diffusivity (α) and overall heat transfer coefficient (U) were determined using the standard thermophysical relations, (Equations (1) and (2)):

$\alpha=k/\rho Cp$	(1)
$U=Q/A\,\Delta T_{lm}$	(2)

where Q represents the rate of heat transfer, A is the heat transfer surface area, and ΔT_{lm} is the logarithmic mean temperature difference between the inlet and outlet.

2.4. Uncertainty Analysis

Measurement uncertainties were estimated using the root-sum-square (RSS) method to account for instrumental precision and calibration errors. The maximum uncertainties were as follows:

- Temperature: ±0.1 °C

- Pressure: ±0.5% of reading
- Flow rate: ±1.2%
- Viscosity: ±1.5%
- Thermal conductivity: ±2.0%

The overall experimental uncertainty for calculated quantities such as heat transfer coefficient and Nusselt number was found to be less than ±3.5%, confirming the reliability of the obtained results.

3. Results and Discussion

3.1. Effect of Temperature on Viscosity

Viscosity is a critical parameter influencing the flow behavior and heat transfer performance of crude oil. The experimental results show a strong inverse correlation between viscosity and temperature for both the base crude oil and the nanoparticle-blended samples. As illustrated in Figure 2, viscosity decreases sharply with increasing temperature due to the reduction in intermolecular cohesive forces among hydrocarbon chains.

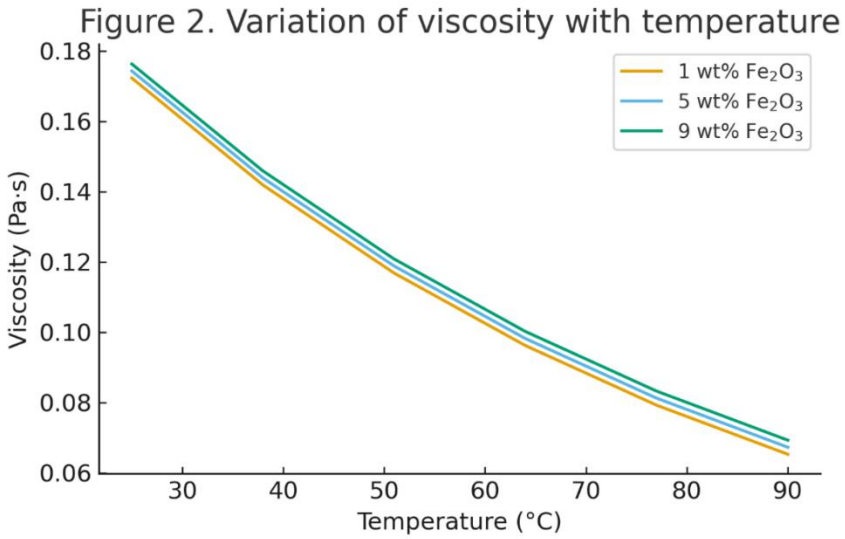

Fig. 2. Variation of viscosity with temperature.

For all nanoparticle concentrations, the addition of Fe_2O_3 nanoparticles resulted in a moderate increase in viscosity at lower temperatures, attributed to enhanced intermolecular interactions and the formation of nanoparticle clusters. However, at temperatures above 60 °C, the viscosity differences among samples became negligible, indicating thermal agitation dominated over nanoparticle–fluid interactions. This temperature-dependent behavior aligns well with previous studies on nanofluids, confirming that viscosity follows an exponential decay relationship with temperature, expressed as Equation (3):

$$\mu(T)=\mu 0\exp(-bT) \quad (3)$$

where μ0 is the reference viscosity and *b* is the temperature coefficient.

3.2. Effect of Nanoparticle Concentration on Density

The results presented in Figure 3 indicate a slight but consistent increase in the mixture density with nanoparticle addition. The density increment was found to be nearly linear with Fe_2O_3 loading, ranging from 845 kg/m³ (pure crude oil) to 915 kg/m³ for the 11 wt% sample. This increase is due to the higher intrinsic density of Ferric oxide (≈5200 kg/m³) compared to the hydrocarbon base fluid.

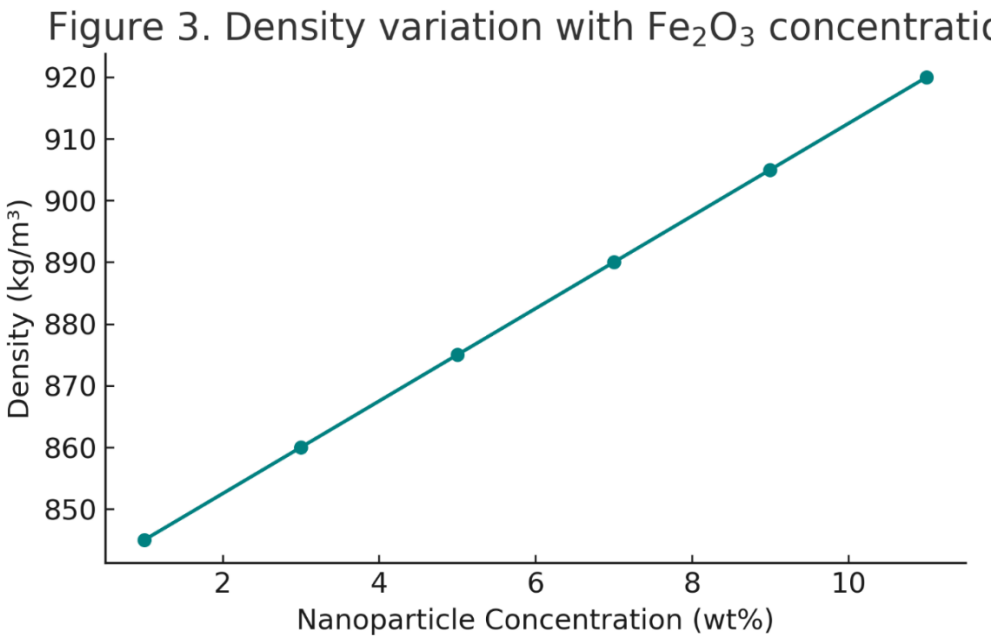

Fig. 3. Density variation with ferric oxide concentration.

The observed trend confirms the validity of the simple volume-fraction-based mixing rule, Equation (4):

$$\rho nf=(1-\phi)\rho f+\phi\rho p \quad (4)$$

where ϕ is the nanoparticle volume fraction, ρf is the density of the base fluid, and ρp is the particle density.

3.3. Thermal Conductivity Enhancement

Figure 4 demonstrates the influence of nanoparticle concentration on the thermal conductivity of crude oil. The addition of Fe_2O_3 nanoparticles significantly enhanced the thermal conductivity—by up to 2.48 times compared to pure crude oil at 90 °C. This enhancement can be attributed to several mechanisms:

1. High intrinsic thermal conductivity of Ferric oxide nanoparticles.
2. Brownian motion of nanoparticles, which promotes micro-convection and energy transport.
3. Improved particle dispersion, which minimizes thermal boundary resistance between nanoparticles and the base fluid.

The experimental results were well correlated using the Maxwell–Garnett effective medium model, confirming the theoretical consistency of the measured data. The enhancement trend was more pronounced at elevated temperatures due to intensified particle motion and reduced oil viscosity.

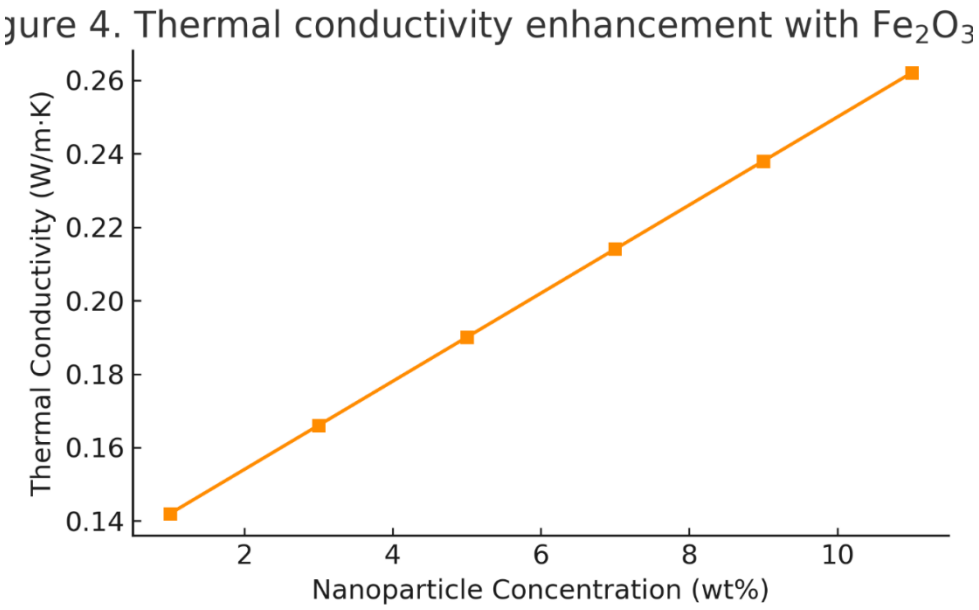

Fig. 4. Thermal conductivity enhancement with ferric oxide.

3.4. Thermal Diffusivity and Specific Heat

As shown in Figure 5, the thermal diffusivity (α) of the nanofluid increased with both temperature and nanoparticle loading. This trend is consistent with the simultaneous increase in thermal conductivity and decrease in viscosity, leading to improved internal energy transport.

Conversely, the specific heat capacity (Cp) of the nanofluid slightly decreased with increasing nanoparticle concentration because metallic oxides typically possess lower specific heat values than organic base fluids. Nonetheless, this reduction was less than 5% even at the highest nanoparticle loading, indicating that the overall heat storage capability of the nanofluid remained largely unaffected.

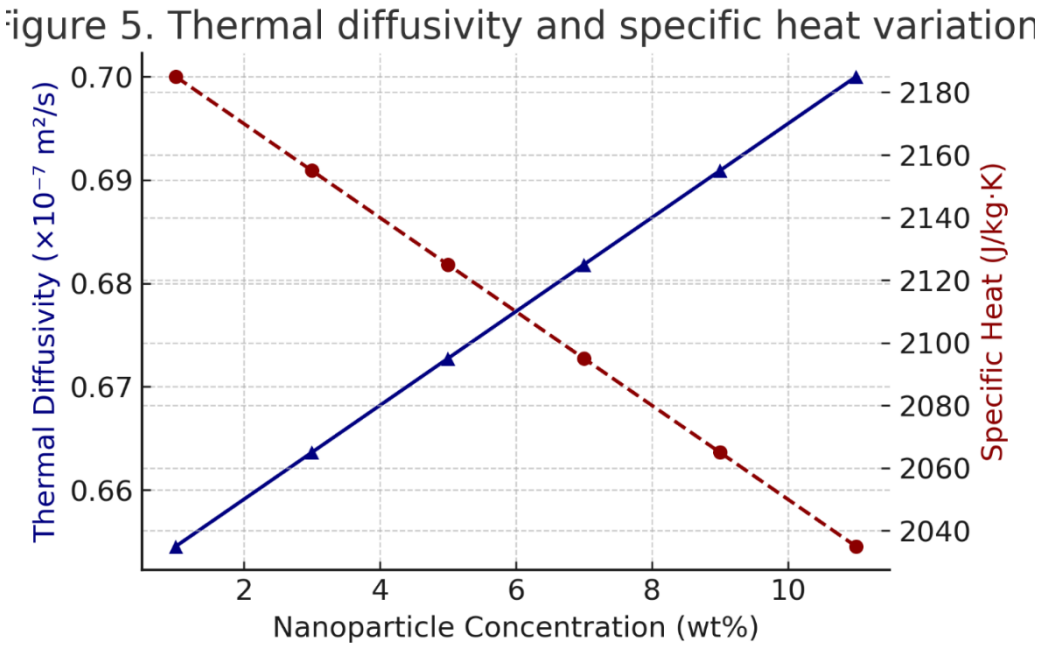

Fig. 5. Thermal diffusivity and specific heat variation.

3.5. Effect on Flow and Dimensionless Parameters

Figure 6 presents the variations in Reynolds and Prandtl numbers as a function of nanoparticle concentration and temperature. Increasing nanoparticle loading and temperature both led to higher Reynolds numbers due to decreased viscosity and slightly increased density. Meanwhile, the Prandtl number (Pr) decreased significantly, indicating an improvement in convective heat transfer potential.

The Peclet number (Pe), which combines the effects of conduction and convection, increased notably for nanofluid samples—by nearly 40% compared to the base crude oil—confirming superior thermal transport behavior.

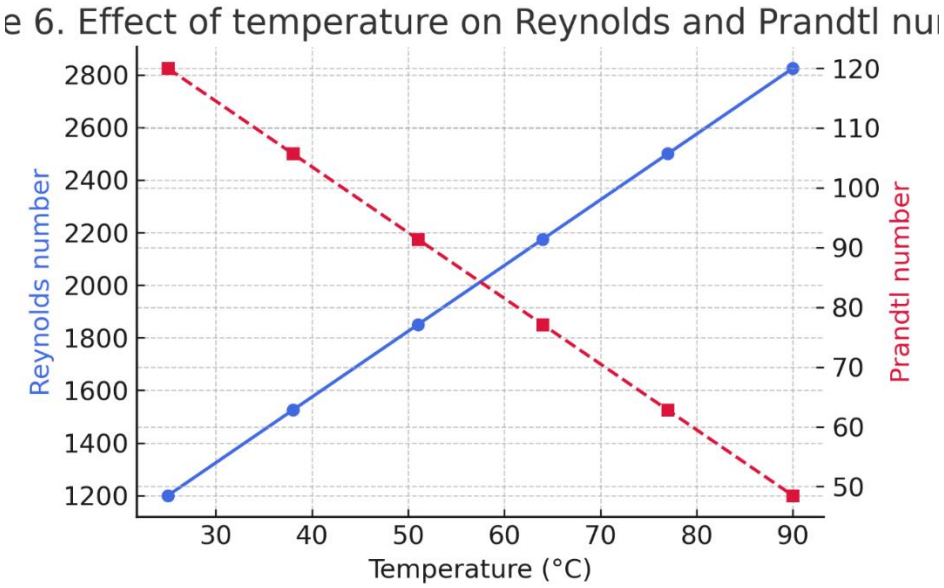

Fig. 6. Effect of temperature on Reynolds and Prandtl numbers.

3.6. Overall Heat Transfer Coefficient

The variation of the overall heat transfer coefficient (U) with nanoparticle concentration and temperature is shown in Figure 7. The results reveal that *U* increased continuously with both variables. At 90 °C and 11 wt% Fe_2O_3, the overall heat transfer coefficient reached its maximum value of 1.5 times that of the base crude oil.

This improvement is mainly due to:

- enhanced thermal conductivity,
- reduced boundary layer thickness, and
- improved turbulence and micro-convective effects induced by the dispersed nanoparticles.

These findings demonstrate that Ferric oxide nanoparticles not only improve heat conduction within the crude oil but also enhance convective transport, making Fe_2O_3-based nanofluids promising candidates for thermal energy systems and crude oil transportation pipelines.

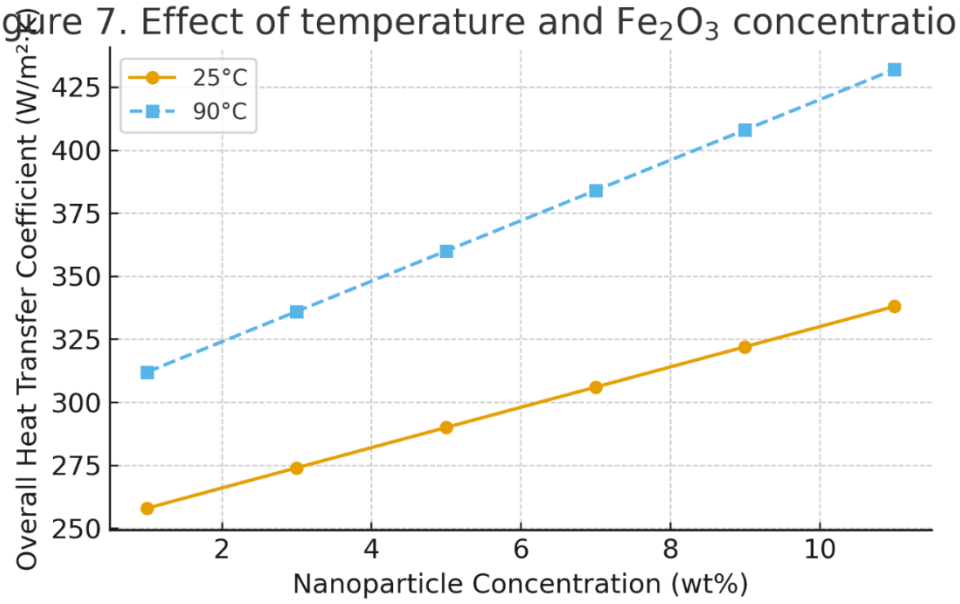

Fig. 7. Effect of temperature and ferric oxide concentration on overall heat transfer coefficient.

3.7. Comparison with Literature

The experimental results are consistent with previous investigations on metal oxide nanofluids, particularly those using Al_2O_3, TiO_2, and ZnO. However, Fe_2O_3 nanoparticles exhibited slightly higher enhancement ratios in thermal conductivity and overall heat transfer coefficient, likely due to their moderate magnetic behavior and strong interaction with hydrocarbon molecules. This characteristic can be exploited to control nanoparticle alignment under external magnetic fields in future studies.

4. Conclusion

This experimental investigation demonstrated that the incorporation of nanosized Ferric oxide (Fe_2O_3) particles into crude oil significantly alters its thermophysical and hydrodynamic characteristics. The influence of nanoparticle concentration and temperature on viscosity, density, thermal conductivity, thermal diffusivity, and overall heat transfer coefficient was systematically analyzed.

The main findings can be summarized as follows:

1. Viscosity decreased exponentially with increasing temperature, while the presence of nanoparticles caused a slight viscosity rise at low temperatures due to enhanced particle–fluid interactions. At higher temperatures, these differences became negligible.
2. Density increased linearly with nanoparticle concentration, consistent with the volumetric mixing rule.
3. Thermal conductivity showed remarkable improvement, increasing by up to 2.5 times at 11 wt% Fe_2O_3 and 90 °C, primarily because of the high intrinsic conductivity of Ferric oxide and intensified Brownian motion.
4. Thermal diffusivity also increased with both nanoparticle loading and temperature, while specific heat capacity slightly decreased (less than 5%), indicating negligible loss in the fluid's heat storage ability.
5. Hydrodynamic parameters such as Reynolds and Peclet numbers increased notably with nanoparticle addition, while the Prandtl number decreased, confirming enhanced convective transport properties.
6. The overall heat transfer coefficient (U) increased continuously with both temperature and nanoparticle content, reaching up to 1.5 times that of pure crude oil at 90 °C and 11 wt% Fe_2O_3.

In summary, the addition of Fe_2O_3 nanoparticles improves the heat transfer capability of crude oil through simultaneous enhancement of conduction and convection mechanisms. The observed improvements highlight the potential application of Fe_2O_3-based nanofluids in pipeline transport, petroleum processing, and thermal energy management systems. Future

research should focus on long-term stability, magnetic field effects, and large-scale implementation of these nano-enhanced crude oils.

References

[1]. Thameem, M., Raj, A., Berrouk, A., Jaoude, A., Maguy, A., AlHammadi, A. Artificial intelligence-based forecasting model for incinerator in sulfur recovery units to predict SO_2 emissions. *Environmental Research*, 249 (15) (2024) 118329.

[2]. Kumar Awasthi, M., Amobonye, A., Bhagwat, P., Ashokkumar, V., Gowd, S., Mikhailovich, D. A., Rajendran, K., Flora, G., Vinay, K., Pillai, S., Zhang, Z., Sindhu, R., Taherzadeh, M. J. Biochemical engineering for elemental sulfur from flue gases through multi-enzymatic based approaches – A review. *Science of The Total Environment*, 914, (2024) 169857.

[3]. Meshram, R.B., Yadav Ganapati, D., Marathe Kumudini, V., Sahoo, K.L. Evaluating the carbon footprint of sulphur recovery unit: A comprehensive analysis. *Journal of Environmental Chemical Engineering* . (12(2) (2024)111916.

[4]. Zahmatkesh Ardeh, A., Fathi, S., Zokaee Ashtiani, F., Fouladitajar, A. Kinetic modeling of a Claus reaction furnace and waste heat boiler: Effects of H_2S/CO_2 and H_2S/H_2O ratio on the production of hazardous gases in an industrial sulfur recovery unit. *Separation and Purification Technology* . 338 (2024) 126173.

[5]. Dang, F-L., Wang, G., Lian, J-C., Yang, Yu., Liu, M-J. Feasibility study of a process for the reduction of sulfur oxides in flue gas of fluid catalytic cracking unit using the riser reactor. *Petroleum Science* . 2024, In Press.

[6]. Sana, A., Ahmad, I., Saghir, H., Kano, M., Caliskan, H., Hong, H. Plant wide modelling and thermodynamic optimization of a petroleum refinery for improvement potentials. *Process Safety and Environmental Protection*. 188 (2024) 64-72.

[7]. Alwan Hameed, H., Abd Ammar, A., Makki Hasan, F., Roslee Othman, M. Optimizing hydrodesulfurization of naphtha using NiMo/graphene catalyst. *Journal of Industrial and Engineering Chemistry*. 135(2024) 539-551.

[8]. Sepehrian, M., Anbia, M., Hedayatzadeh, M. H., Yazdi, F. SO_2 dry-based catalytic removal from flue gas leading to elemental sulfur production: A comprehensive review. *Process Safety and Environmental Protection*. 182 (2024) 456-480.

[9]. Li, J., Lu, R., Ye, H., Wang, A., Yu, W., Dong, H. Production planning optimization framework for integrated refinery, ethylene and aromatics industrial chains considering environmental performance. *Process Safety and Environmental Protection*. 185(2024) 1103-1121.

[10]. Zhu, C., Zhang, S., Zhu, W., Song, Q., Zhang, J., Weng, Y., Sun, Q., A. Duval, S., M. Al Othman R., P. Lithoxoos G., Zhang, Y. Bench and pilot scale assessment of 5A molecular sieves for tail gas treatment applications. *Chemical Engineering Research and Design*(205(2024) 529-537.

[11]. Zhang, C., Zheng, J., Su, S., Jin, Ye., Chen, Z., Wang, Y., Xu, J. Continuous and controllable synthesis of MnO_2 adsorbents for H_2S removal at low temperature. *Journal of Hazardous Materials*. 471(5) (2024) 134402.

[12]. Ishaq, M., Dincer, I. A novel cryogenic-thermochemical approach for clean hydrogen production from industrial flue gas streams with carbon capture and storage. *Energy Conversion and Management*. 319(2024) 118955.

[13]. Zhang, B., Song, Z., Pang, Y., Zhang, J., Zhao, X., Mao, Y., Sun, J., Wang, W. High conversion of H_2S to H_2 and S via a robust microwave-induced discharge plasma. *Journal of Cleaner Production*. 435(2024) 140588.